2017

# Experimental Study of Frequency Oscillations in Islanded Power System

Kevin Daniel Wellman
*Louisiana State University and Agricultural and Mechanical College*, kwellm1@lsu.edu

# EXPERIMENTAL STUDY OF FREQUENCY OSCILLATION IN ISLANDED POWER SYSTEM

A Thesis

Submitted to the Graduate Faculty of the
Louisiana State University and
Agricultural and Mechanical College
in partial fulfilment of the
requirements for the degree of
Master of Science in Electrical Engineering

in

The Department of Electrical and Computer Engineering

by
Kevin Daniel Wellman
B.S., Mississippi State University, 2011
August 2017

## ACKNOWLEDGEMENTS

I would like to thank Louisiana State University and Entergy Corporation for funding this project. I would also like to thank Dr. Shahab Mahraeen for teaching and the wealth of information he gave to me. I would also like to thank Pooria Mohammadi and other students for the assistance while working on the experiments.

**TABLE OF CONTENTS**

## ABSTRACT

Since the introduction of power electronics to the grid, the power system has quickly changed. Fault detection and removal is performed more accurately and at quicker response time, and non-inertia driven loads have been added. This means stability must continue to be a main topic of concern to maintain a stable synchronized grid.

In this thesis a lab was designed, constructed, and tested for the purpose of studying transient stability in power systems. Many different options were considered and researched, but the focus of this paper is to describe the options chosen. The lab must be safe to operate and work around, have flexibility to perform many different type of experiments, and accurately simulate a power system.

The created lab was then tested to observe the impact of PSS on an unsynchronized generator connected to a static load. The lab performed as designed, which allows for the introduction of more machines to create the IEEE 14 Bus grid.

# CHAPTER 1: INTRODUCTION

## 1.1 Introduction

The first power grid was built in England in 1881, with numerous patents created in the following years. Thomas Edison insisted on a Direct Current system, but this proved to be inefficient due to high line loss at low voltage levels. It was not until the 1930's when power electronics were created to simplify voltage transformations on DC systems. Instead, the grid was designed for Alternating Current by utilizing Nikola Telsa's patents on transformers and induction motors. The world electrical demand has grown to nearly 23,000 TWh/year according to the International Energy Agency. Electricity not only provides comfort and entertainment, but more importantly, sustaining life.

Stability, a system's ability to return to equilibrium after a disturbance, is a key component necessary for reliable operation of any system. In the 1920's, damping was solved by introducing generator damper windings and changing prime mover design to turbine style. Since the introduction of power electronics, the grid has quickly evolved and become more complicated. Modern systems contain non-inertia driven equipment and components incapably of supplying reactive power. The response time to an event must be decreased to maintain stable operation. Generator stability can be broken down into three main categories: steady-state, transient, and dynamic.

Steady state instabilities occurs in the time periods of 0 to $10^{-3}$ seconds. These include lightning and switching surges and stator transients and sub-synchronous resonance. Due to

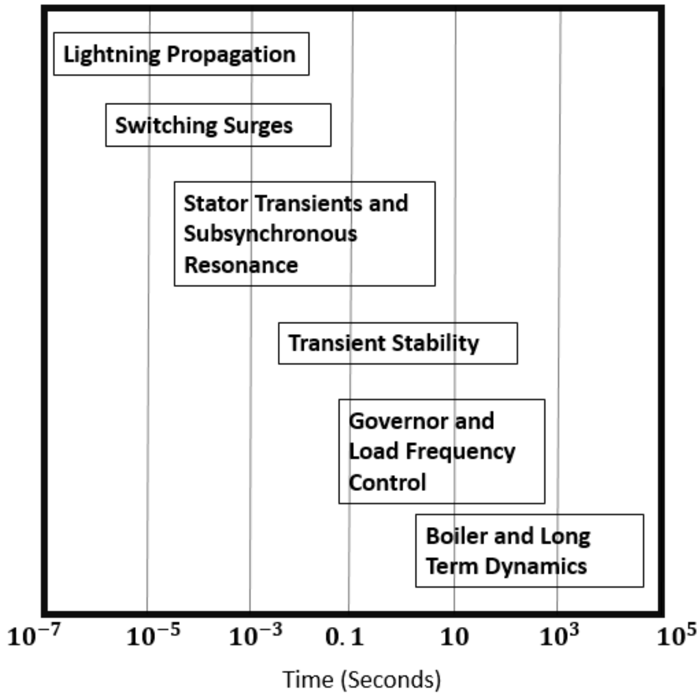


Figure 1.1: Power System Instability

the high response time required, passive components such as Metal-Oxide Varistor arrestors or capacitors are utilized. These components chop waveform peaks and smooth out the corresponding oscillations.

Transient stability occurs in the time period of sub-seconds to tens of seconds. These disturbances are caused by fluctuation in load or generation. A synchronous power system must operate at equilibrium, meaning generation must always equal consumption. Consumption includes energy used to drive rotating equipment, line losses, and faults. When load is added, frequency decreases and inertia of the generator supplies the additional load. Additional energy must be then supplied to the prime mover to keep the system in equilibrium. The dampening of these oscillation generally occurs by synchronous machine dynamics or power electronics component compensation. Systems such as a Power System Stabilizer can increase the damping ability of a generator.

Dynamic stability is a slow response requiring tens of seconds to minutes of time. These stabilizers are used to control load fluctuations by reducing energy created by the generator prime mover. Examples would include adjusting fuel delivered to boiler for steam driven equipment, regulating fuel delivery to combustion driven generators, or modifying the pitch of wind powered generators.

System studies can be performed by using advanced software, but at times, a physical model may need to be created in order to validate the results. The LSU Generator Stability Lab was designed to handle a variety of experiments. These experiments may be performed synchronized to the grid or isochronous. Photovoltaic cells and inverters are included in the lab to be able to model a micro grid or grid containing only non-inertia driven power sources. A key component of a university is creating a learning environment for faculty and student. The lab creates unique opportunity for fostering education through use of a small scale power system. Topics can be focused on stability, fault analysis, protection systems, PV integration, harmonics, or motor dynamics.

This paper description the purpose for the lab, selection of components, integration of system, and frequency oscillations in an islanded system. Many different options were evaluated, but the focus of this paper is to discuss the designed system.

# CHAPTER 2: THEORETICAL BACKGROUND

## 2.1 Transient Stability

Although the power system may be considered a robust system of networks connected over thousands of miles, oscillations are continuously observed. These can be presented as frequency or voltage related. Elimination of the initiator is viewed as unrealistic, since it may be in the form of lightning impulses, load oscillations, or faults. Transients in the power system are caused by large disturbances, such as faults, loss of generation, or sudden load changes. The power angle is used to determine whether the machine can return to steady-state operation after a transient occurs.

The rotor motion is defined by Newton's second law.

$$J\frac{d^2\theta}{dt^2} = T_m - T_e = T_\alpha \quad (2.1)$$

Where

$$\mathrm{J} = \text{ total moment of inertia of the rotating mass}, kgm^2$$

Θ = angular position of the rotor in rad

$$T_m = mechanical\ torque\ supplied\ by\ the\ prime\ mover\ minus$$
$$the\ retarding\ torque\ due\ to\ mechanical\ loss, Nm$$
$$T_e = electrical\ torque\ that\ accounts\ for\ the\ total\ three\ phase\ electrical\ power\ output$$
$$of\ the\ generator, plus\ electrical\ loss, Nm$$
$$T_a = Net\ accelerating\ torque, Nm$$

Inertia constant is then normalized to:

$$H = \frac{Stored\ Kinetic\ Energy\ at\ Synchronous\ Speed(Mega\ Joules)}{Generator\ MVA\ Rating} = \frac{J\ \omega_2^2}{2S_{Rated}} \quad (2.2)$$

Per unit swing equation is defined as the following:

$$\frac{2H}{\omega_s}\left(\frac{d^2\delta(t)}{dt^2}\right) = P_m(t) - P_e(t) = P_a(t) \quad (2.3)$$

Where $\delta = power\ angle$

Swing equation can then be converted to two 1st order derivatives.

$$\frac{\mathrm{d}\Delta\omega_r}{\mathrm{dt}} = \frac{2}{2H}(P_m - P_e) \qquad (2.4)$$

$$\frac{\mathrm{d}\delta}{\mathrm{dt}} = \omega_{sm} x \Delta\omega_r) \qquad (2.5)$$

The power angle is the angle between the generator internal and terminal voltage phasor. Every machine has a critical angle in which if this angle is surpassed, then the machine can never return to a steady state. The equal area criterion is used to describe a machine's response to transients. Equal Area Criterion is broken down into three distinct time periods: $A_1$ $i$s pre-fault, $A_2$ is during the fault, and $A_3$is post-fault. When areas under the curve are equal, the machine is in equilibrium and stable.

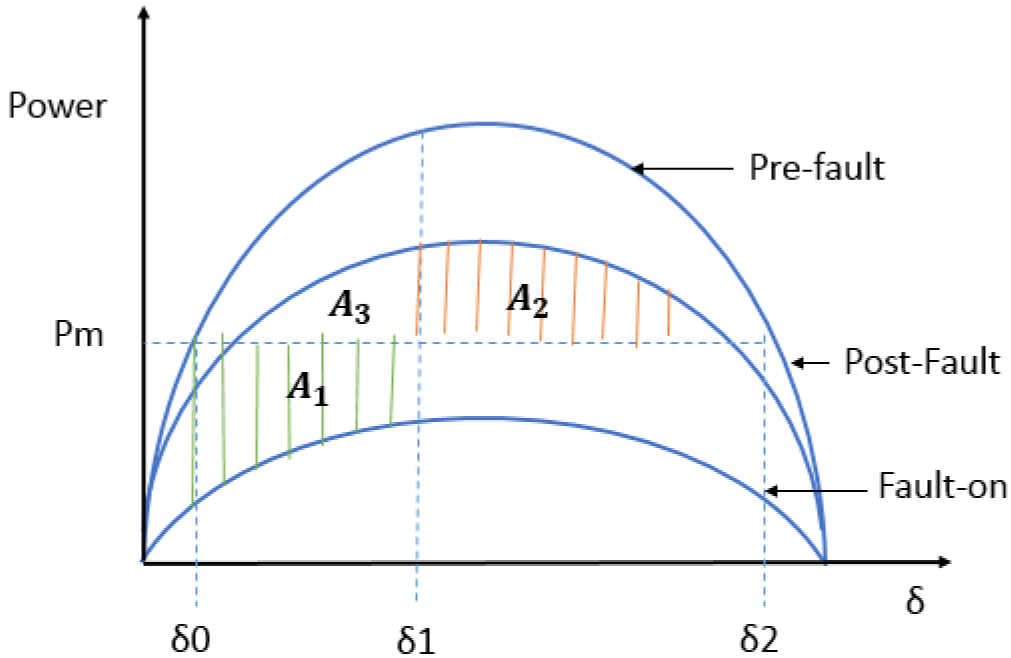


Figure 2.1: Equal Area Criterion Chart

$$A_1 = \int_{\delta_0}^{\delta_{cl}} (P_m - P_{ef}\sin(\delta))\, d\delta \quad (2.6)$$

$$= \int_{t_0}^{t_{cl}} \mu\, \frac{d\omega}{dt} x\, \omega\, dt$$

$$= \frac{1}{2}\mu\, \omega_{cl}^2 = Kinetic\ Energy$$

$$A_2 = \int_{\delta_{cl}}^{\delta_u} (P_{e\,pf}\sin(\delta) - P_m)\, d\delta \quad (2.7)$$

$$= \int_{\delta_{cl}}^{\delta_u} \mu\, \frac{d\omega}{dt}\, d\delta$$

$$= -[\frac{1}{2}\mu\, \omega_u^2 - \frac{1}{2}\mu\, \omega_{cl}^2]$$

$$= Potential\ Energy = Energy\ to\ be\ Absorbed\ by\ the\ System$$

$$A_3 = \int_{\delta_d}^{\delta_{cl}} (P_{e\,EE}\sin(\delta) - P_m)\, d\delta \quad (2.8)$$

$$= \int_{\delta_d}^{\delta_{cl}} \mu\, \frac{d\omega}{dt}\, d\delta$$

$$= -[\frac{1}{2}\,\mu\,\omega_{cl}^2 - \frac{1}{2}\,\mu\,\omega_d^2]$$

Transient Energy Function is now defined as:

$$V(\delta, \omega) = \frac{1}{2}M\omega^2 - P_m(\delta - \delta_s) - P_{e\ PF}\,(\cos\delta - \cos\delta_s) \qquad (2.9)$$

Then

$$A_2 + A_3 = V(\delta_u, 0) = A_1 + A_3 = V(\delta_{cl}, \omega_{cl}) \qquad (2.10)$$

**2.2 Generator Model**

Synchronous generator dynamic models are used to confirm system stability and predict post fault quantities. For this paper, three different models will be discussed. The higher complexity leads to more precise modeling, and the one axis model is used for PSS control.

Classical model is the least complex of all, and is sufficient for analyzing swing stability. The classical model consists of a constant voltage source and subtransient reactance. This model is best utilized when observing response to an event on an infinite bus.

One axis model includes the d axis, whereas the two axis model adds the d and q axis. For a rotating field to exist, there must be a three phase voltage present in the stator windings, and the stator windings are considered to be sinusoidally distributed. D axis is in the direction of the rotor DC magnetic field, and q axis is perpendicular. Q axis includes damper windings known as ammortisseur. Inductances and reluctances between the axis’ are completely separate.

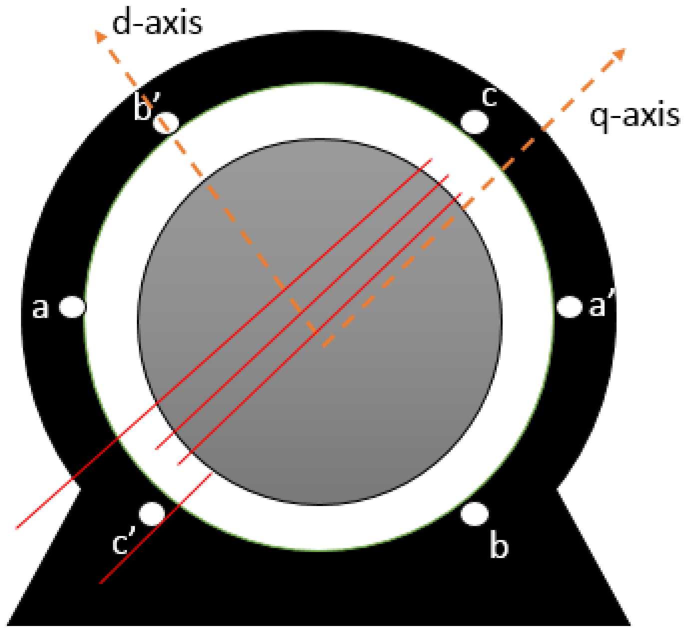


Figure 2.2: Synchronous Machine dq Axis Diagram

One axis model is created by utilizing the equivalent circuit in Figure 2.3. From there, algebraic equations are converted to form dynamic equations. Generator datasheets contain necessary information to obtain machine resistances and reactances.

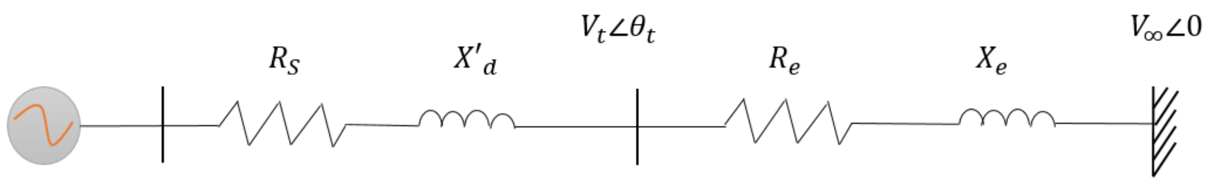


Figure 2.3: One Axis Equivalent Circuit

$$\dot{E}'_q = -\frac{1}{T'_{d0}}\left(E'_q + (X_d - X'_d)I_d - E_{fd}\right) \quad (2.11)$$

$$\dot{\delta} = \omega - \omega_s \quad (2.12)$$

$$\dot{\omega} = \frac{\omega_s}{2H}(P_m - (E'_q I_q + (X_q - X'_d) I_d I_q \qquad (2.13)$$

$$0 = R_s I_d - X_q I_q + V_d \qquad (2.14)$$

$$0 = R_s I_q + X'_d I_d + V_q - E'_q \qquad (2.15)$$

$$0 = R_e I_d - X_e I_q - V_d + V_\infty sin\delta \qquad (2.16)$$

$$0 = R_e I_q + X_e I_d - V_q + V_\infty cos\delta \qquad (2.17)$$

Model can then be linearized to form equation 2.18. Damping of oscillations occur by controlling inputs, $P_{mi}$ and $V_{ref}$.

$$0 = [A_1] \begin{bmatrix} \Delta E'_{qi} \\ \Delta \delta_i \\ \Delta \omega_i \\ \Delta E_{fdi} \end{bmatrix} + [B_{11} \vdots B_{21}] \begin{bmatrix} \Delta y'_i \\ \Delta y''_i \end{bmatrix} + C_{11} \begin{bmatrix} \Delta P_{mi} \\ \Delta V_{ref} \end{bmatrix} \qquad (2.18)$$

**2.3 Design of PSS**

Since oscillations are present on most systems, dampeners must be designed and installed to reduce the impact. When dampeners are inadequate, the oscillations will increase until the system is unstable and unable to resolve itself.

Oscillations in power systems may be caused by the generator and prime mover or by an outside source. Rotor dynamics and turbine load swings are examples of oscillations caused by the machine. Whereas other machines on the power systems, electrical fault, or load changes can produce these disturbances. Fast response to disturbances greatly improves the reliability of the systems.

A turbine driven generator has several different methods to dampen oscillations. A Power System Stabilizer (PSS) utilizes the voltage regulator to dampen electromechanical oscillations. PSS manipulates the electric torque to stabilize the shaft speed and return it to a stable system. PSS utilizes 2 key quantities: shaft speed and electrical power.

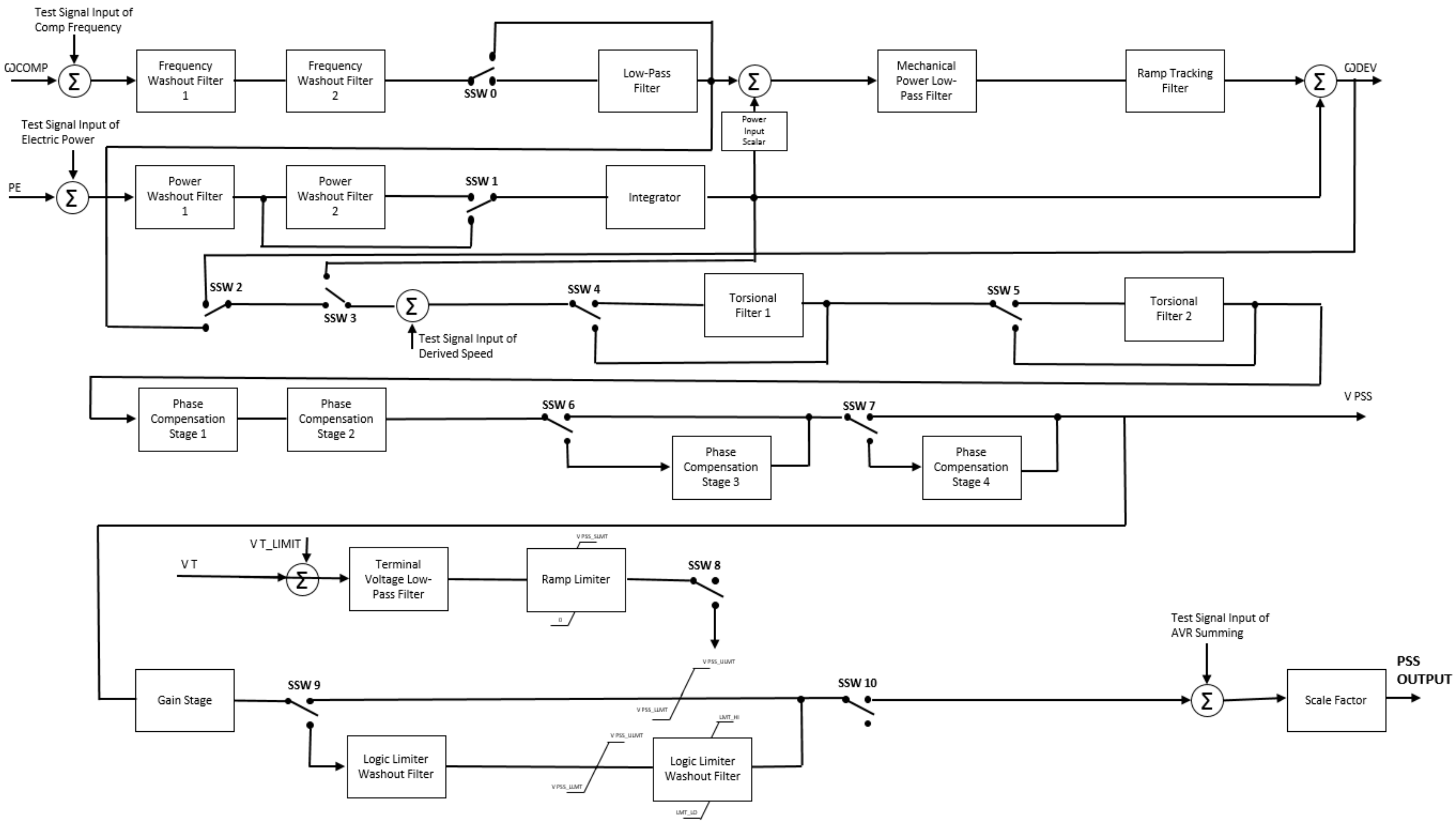


Figure 2.4: IEEE AVR Block Diagram [3]

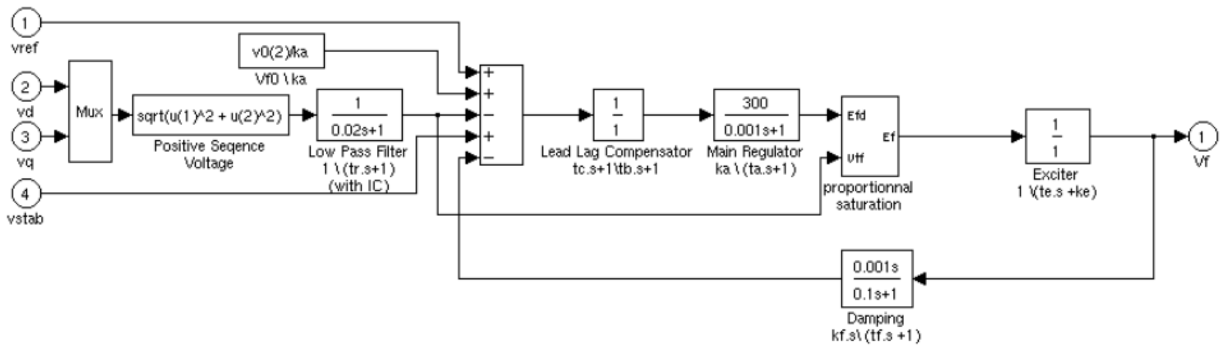


Figure 2.5: Simulink AVR Exciter Block Diagram

The exciter is represented by the following transfer function between the exciter voltage, Vfd and the regulator's output, ef.

$$\frac{Vfd}{ef} = \frac{1}{\mathrm{Ke+sTe}} \qquad (2.19)$$

# CHAPTER 3: POWER SYSTEM DESIGN

## 3.1 Motor Generator Set

The LSU Generator Stability Lab was designed to handle a variety of experiments including generator stability, PV system integration, and micro-grid design. The main components of this lab are the generator, prime mover, loads, and respective control systems. Motor generator (MG) set was specified and purchased for the lab. The main constraint was to operate at a lower speed and voltage for safety reasons, but also a high enough level to properly perform experiments. The lab operates at 240V 3 phase 60Hz and the MG set is rotating at 1800 rpm. The system was designed to be mobile, by adding casters to all equipment, to allow more flexible for future experiments.

The generator is a brushless synchronous machine directly coupled to an induction motor, which serves as the prime mover. The generator and motor are 4 pole air cooled machines rated for 7.2kVA. The Non Drive End of the generator houses an incremental encoder for speed reference. Encoder utilizes 3 channels at 360 pulses per revolution which allows precise speed measurement, but also rotor position within 45°.

Generator impedance switch was created to change the impedance of the generator. This allow the machine to operate in parallel impedance wye or single impedance wye. Thermal magnetic breaker are included to ensure generator is not damaged during operation.


Figure 3.1: MG Set with Flywheel

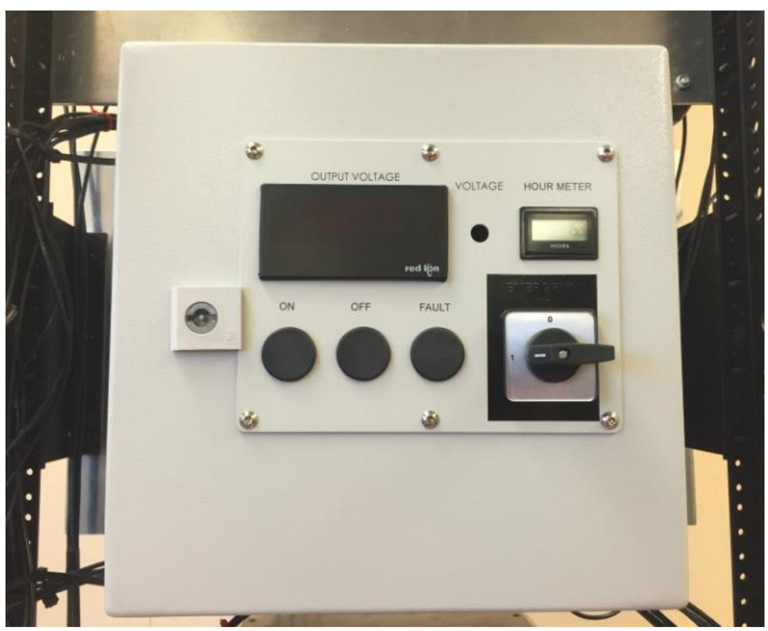


Figure 3.2: Generator Impedance Switch

### 3.2 Inertia Calculation

Industrial steam turbines and gas turbines have a high inertia value due to the rotating mass and high speed operation. This help to dampen oscillations and continue to provide power during transient events. Flywheels were needed to increase the inertia of the motor generator set to better simulate a steam or gas turbine operation. Two flywheels were designed and manufactured. Thus, the flywheels were specified with an H =1 and H = 5. Listed below are the formulas used to provide the specification of the flywheels.

$$H = 0.5\, J\, (\omega_b \times \frac{2}{\pi})^2 / S_b \quad (3.1)$$

$$J = (\mathrm{M} \times r^2)/2 \quad (3.2)$$

$$Volume = \pi \times r^2 \times h \quad (3.3)$$

Table 3.1: Motor and Generator Inertia at Synchronous Speed (1800 rpm)

| | |
|---|---|
| Generator H | 0.052 kg $m^2$ |
| Motor H | 0.040 kg $m^2$ |

Lab requirement mandated the flywheels to be easily changeable, so weight was a concern. Tapered hubs were chosen to be welded in the flywheel due to exceptional shaft compression and ease of removal. High speed balancing was performed on the flywheel assembly. Flywheel was mounted on a 1 3/8” shaft and directly coupled to the motor Non Drive End by way of a jaw type coupling with an elastomer. This type of coupling helps to dampen vibrations and noise caused by misalignment, bearing wear, or imbalance, by dampening across the coupling. Shaft is supported on two pillow block bearings.

Table 3.2: Flywheel Specifications

| Flywheel Types | Thickness | Radius | Weight |
|---|---|---|---|
| H =1 | 0.6” | 7.95” | 33.79 lbs |
| H =5 | 0.6” | 12.54” | 84.05 lbs |

### 3.3 Control Mechanism

In order to control a single generation unit, many different control devices must operate in conjunction with each other. Control components were mounted on a single rack with casters.

The generator was equipped with a voltage regulator, but this was disconnected due to the lack of flexibility. A Basler DECS-250 was purchased to control the generator field. This was purchased without the Power Systems Stabilizer module. The generator can be operated in 2 basic modes, Automatic Voltage Regulation (AVR) or Manual. AVR monitors and maintains the generator terminal voltage. Manual keeps the field current or voltage, depending on the control method, constant regardless of bus voltage or load changes. Inputs include generator terminal voltage, generator current, trip command from relay, and PSS gain from dSPACE . The only outputs is DC current to generator brushless field.

Figure 3.3: Motor and Generator Controls

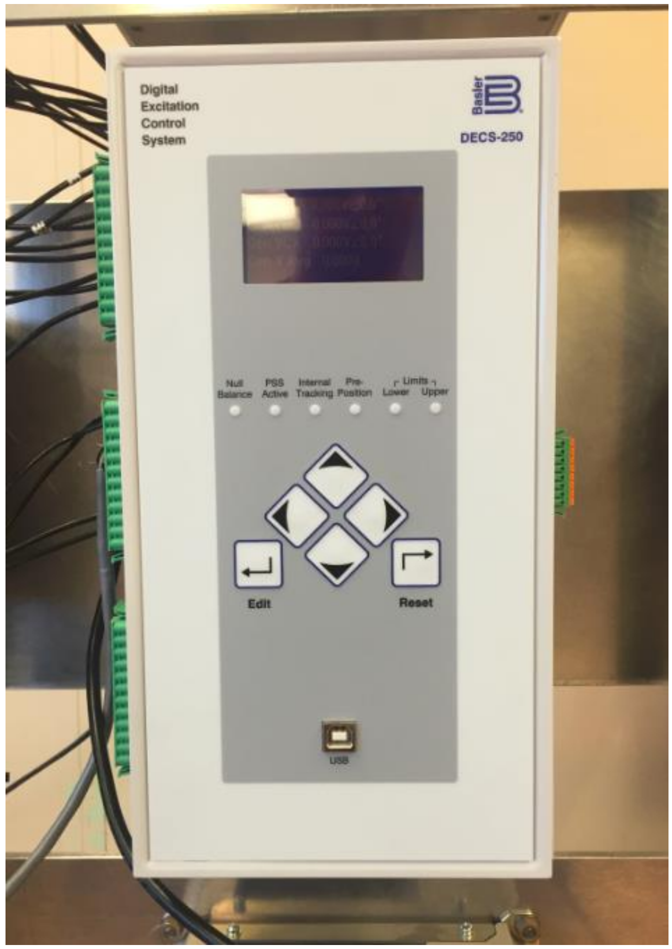


Figure 3.4: Generator Voltage Regulator

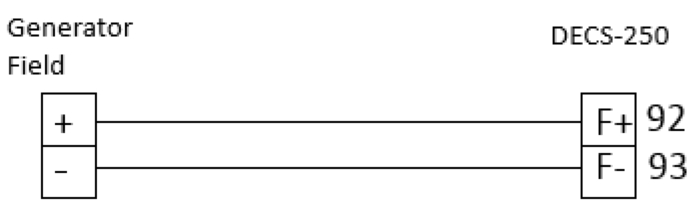


Figure 3.5: Generator Field Loop Diagram

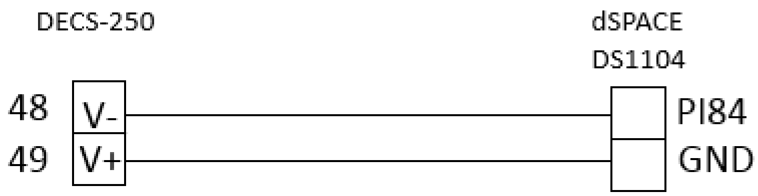


Figure 3.6: PSS Gain Loop Diagram

The generator is protected by way of a Beckwith 11G relay with high accuracy Current Transformers (CT). ABB CMF-S were purchased for phase and neutral current CT's. Addition turns were made through the CT's to lower the effective ratio, which increases the secondary current. Generator terminal voltage and current inputs are sent to the relay as inputs. Output consists of trip command to voltage regulator, generator contactor, and VFD.


Figure 3.7: Generator Protection Relay

The induction motor servers as the prime mover for the generator. A speed control system is needed to keep the motor at synchronous speed. Induction motor speed is characterized by equation 3.5.

$$n = n_1\,(1 - s) \qquad (3.5)$$

$$where$$

$$n = Speed\ of\ Rotor\ (RPM)$$

$$n_1 = \text{Speed of Magnetic Flux (RPM)}$$

$$s = Slip\ (RPM)$$

To combat the inherent slip and speed reductions caused by increased loading, a Variable Frequency Drive was installed. A 480V VFD was specified, so a step up transformer was purchased to accommodate the lower voltages present in the lab. PID control loop was installed with an encoder to keep the machine at synchronous speed. Input to PID control is the generator quadrature encoder.

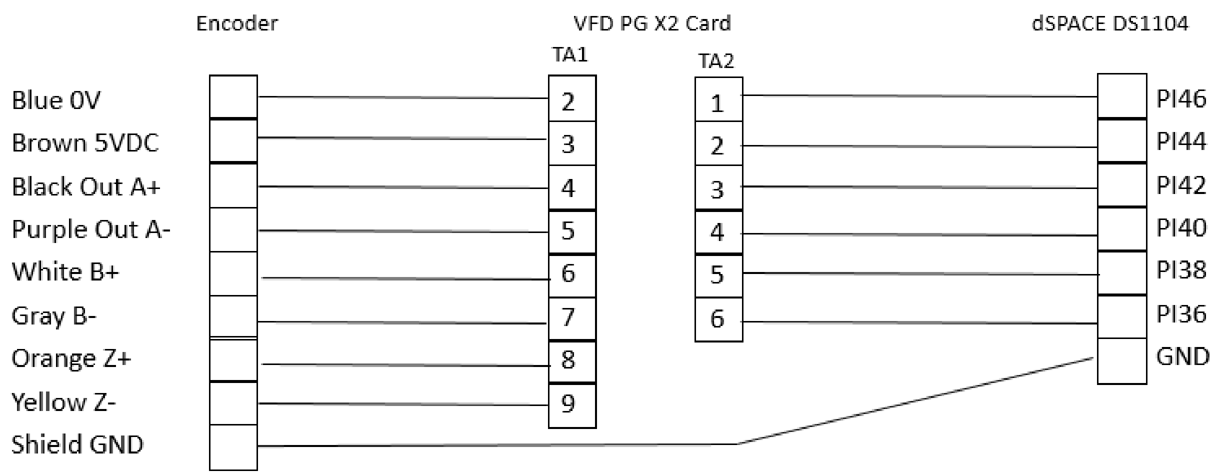


Figure 3.8: Speed Signal Loop Diagram

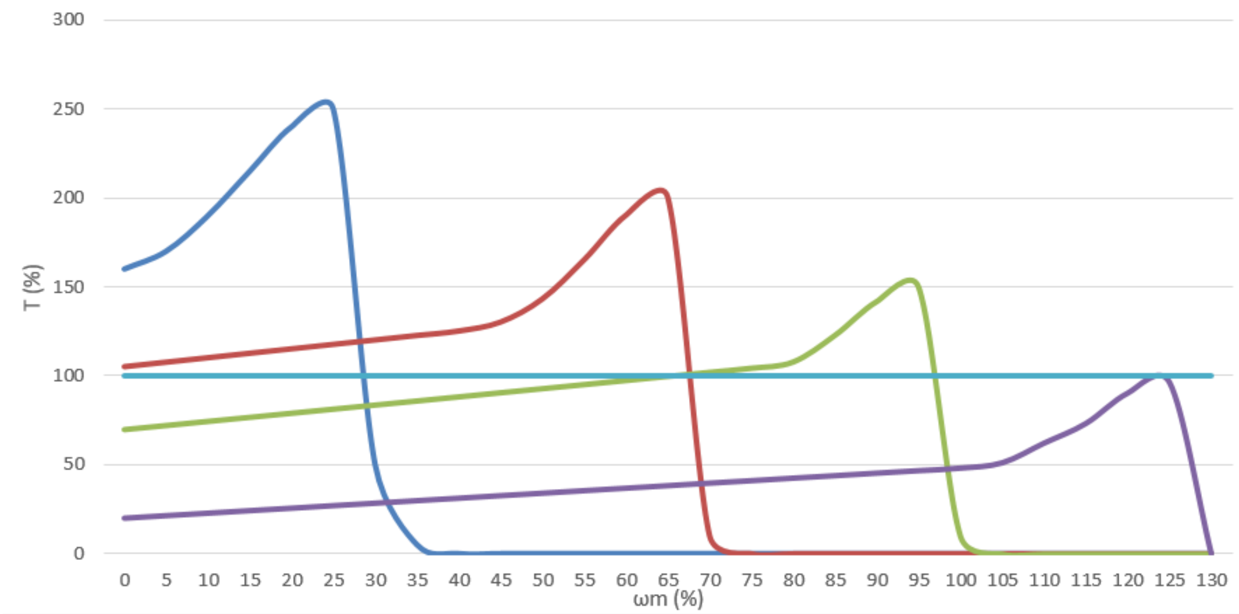


Figure 3.9: Torque versus Speed on Variable Frequency Control

A VFD controls the speed of the motor similarly to a gas or steam turbine powered generator. Multiple control modes can be utilized and key variables can be adjusted to change the performance of the prime mover. Flux Vector control was chosen due to precise speed and torque control as well as feedback utilization. The encoder signal is sent to the VFD as a reference value.

### 3.4 Power System Stabilizer

The Simulink Generic Power System Stabilizer was implemented via dSPACE to show proof of concept. The PSS utilizes a single speed deviation input and exports a stabilized voltage per unit value to send to the voltage regulator as a $\pm$ 5VDC. The voltage regulator then interprets this as a gain function to adjust the generator terminal voltage to. Voltage regulator controls the DC field current of the synchronous generator. As generator terminal voltage decrease, electric power delivered from the generator decreases as well.

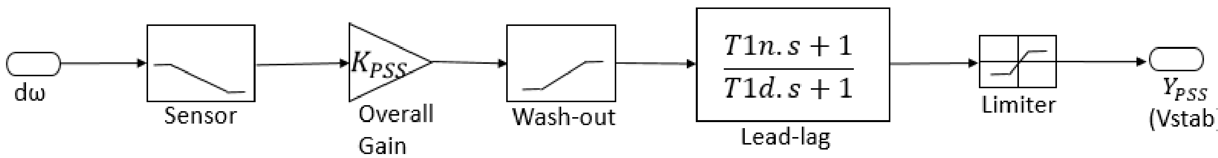


Figure 3.10: Simulink PSS Block Diagram

PSS was executed in dSPACE by reading and determining speed from the quadrature encoder. Speed deviation is amplified by to increase the sensitivity of PSS control through a gain block. Wash-out is a low pass filter designed to remove harmonics above fundamental. Lead-lag provides phase lead compensation to account for inherent phase lag. Limiter is used to keep the PSS control from excessive manipulator of generator terminal voltage.

$\Delta Y_{PSS}$ in equation 3.6, is added into the voltage regulator signal, and A Matrix is modified to create equation 3.8.

$$\Delta E_{fd} = \frac{K_A}{1+sT_A}(\Delta V_{ref} - \Delta V_T + \Delta y_{PSS}) \qquad (3.6)$$

$$\Delta \dot{y}_{PSS} = -\frac{1}{T_2}\Delta y_{PSS} + \frac{K_{PSS}}{T_2}\frac{\Delta\omega}{\omega_s} + \frac{T_1 K_{PSS}}{T_2}\frac{\Delta\dot{\omega}}{\omega_s} \qquad (3.7)$$

$$\Delta \dot{y}_{PSS} = -\frac{1}{T_2}\Delta y_{PSS} + \frac{K_{PSS}}{\omega_s T_2}\Delta\omega + \frac{T_1 K_{PSS}}{2HT_2}(\Delta P_m - K_1\Delta\delta - K_2\Delta E'_q) \qquad (3.8)$$

PSS constants are then chosen by utilizing an arbitrary number for $T_2$ and performing equations 3.9 and 3.10. $K_{PSS}$ is typically set higher than the calculated value, but this gives a good starting point before commissioning.

$$T_1 = \frac{\tan(tan^{-1}(\omega T_2) - \varphi_{PSS})}{\omega} \quad (3.9)$$

$$K_{PSS} = \frac{1}{|G_{PSS}(j\omega)||H(j\omega)|} \quad (3.10)$$

### 3.5 Transmission Lines and Loads

The lab grid is modeled after the IEEE 14 bus arrangement shown in Figure 3.8, whereas the impedance matrix is shown in Appendix A. Lines and load can be created by utilizing capacitors, iron core inductors, and high resistance wire.

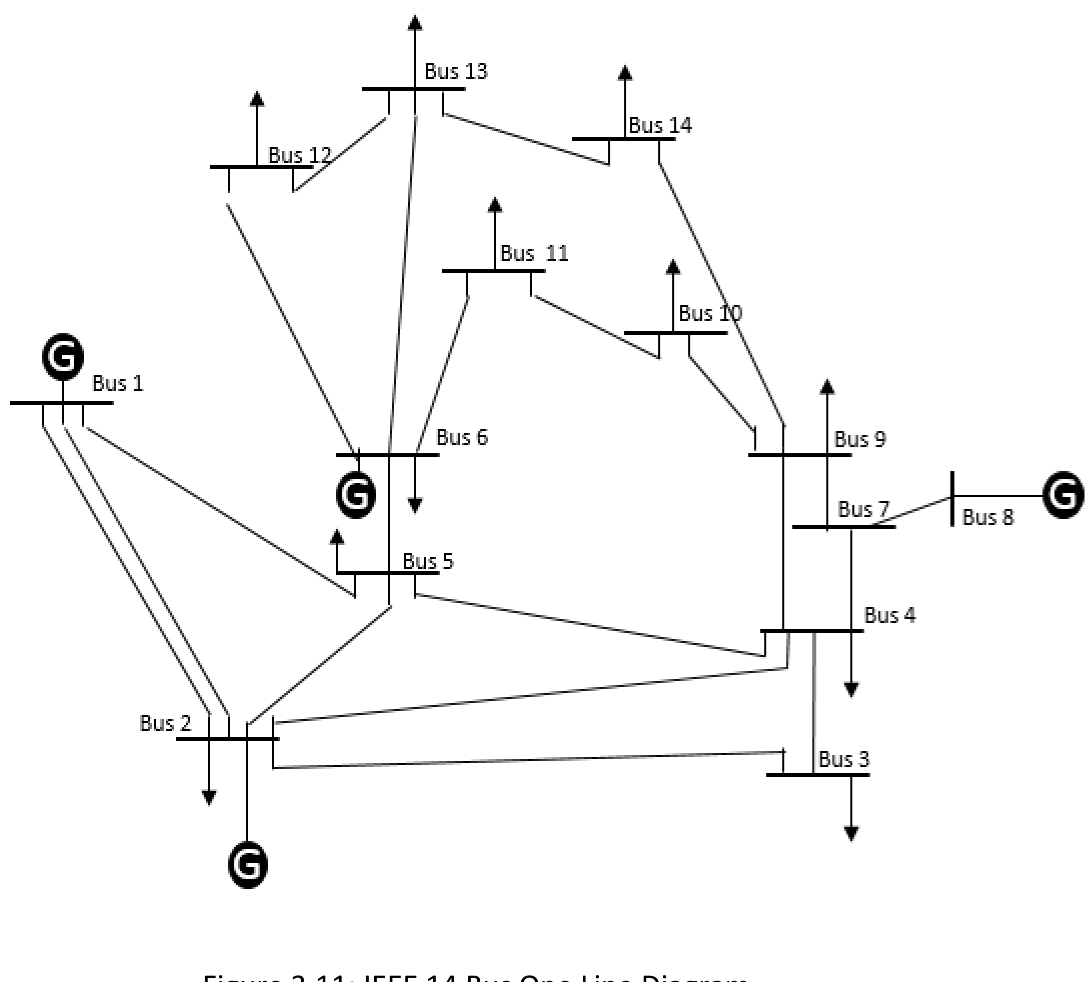


Figure 3.11: IEEE 14 Bus One Line Diagram

### 3.6. Photo Voltaic Cells

A PV system was specified to connect to the lab system. The system must operate in the off-grid and on-grid modes. This requires a battery system to be connected in order to supply power during times where power production momentarily dips to low levels, such as when a cloud passes overhead. To better model typical PV generation, single phase inverters with a wide range of control options were selected.

# CHAPTER 4: EXPERIMENTS

## 4.1 Simulation Model

A software model was created to replicate the physical lab model. Simulink has an excellent library of devices. Figure 4.1 shows the full model with includes the VFD, motor, generator, voltage regulator, and PSS. Scopes were added to display trends.

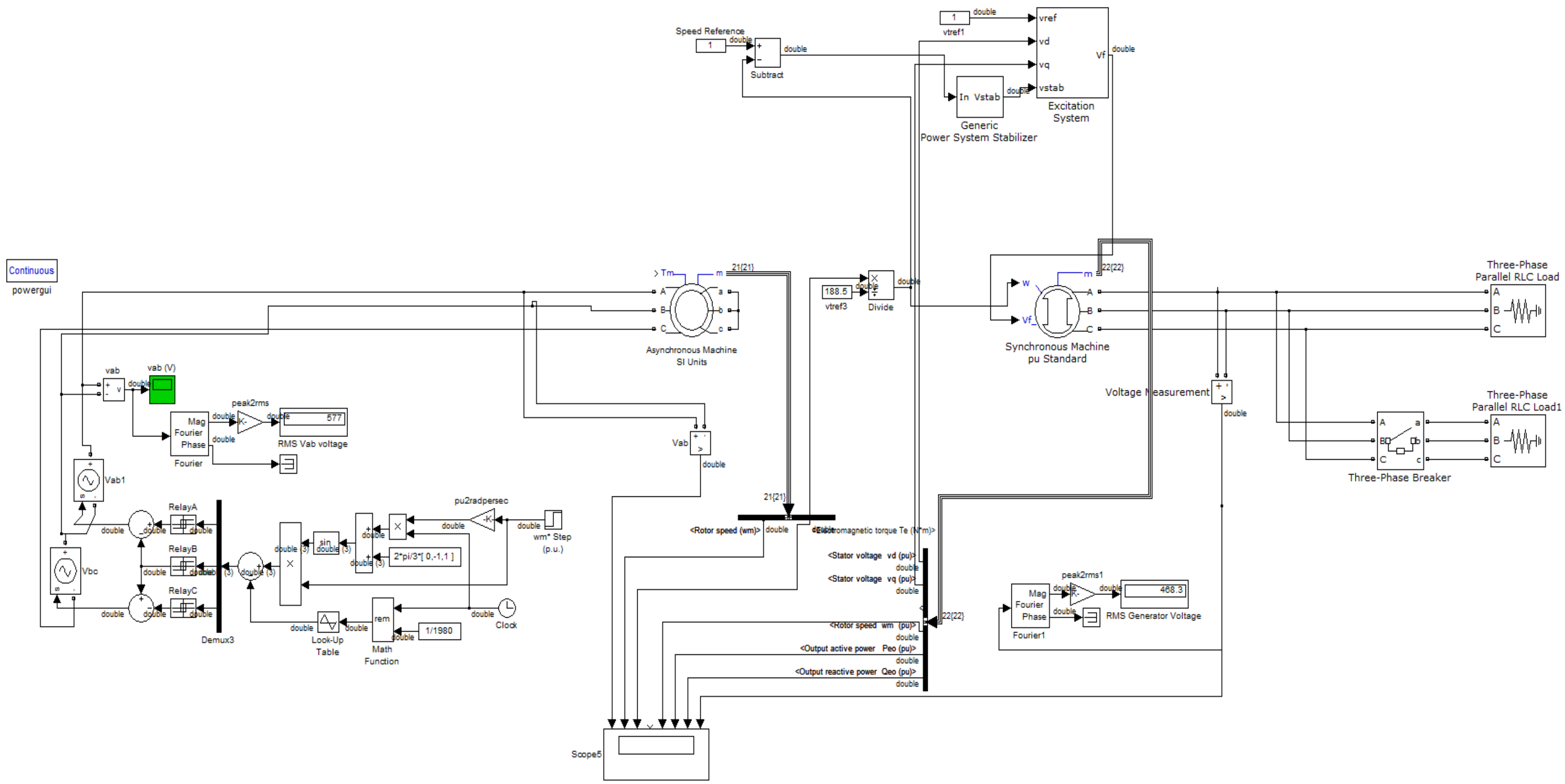


Figure 4.1: Simulink Block Diagram

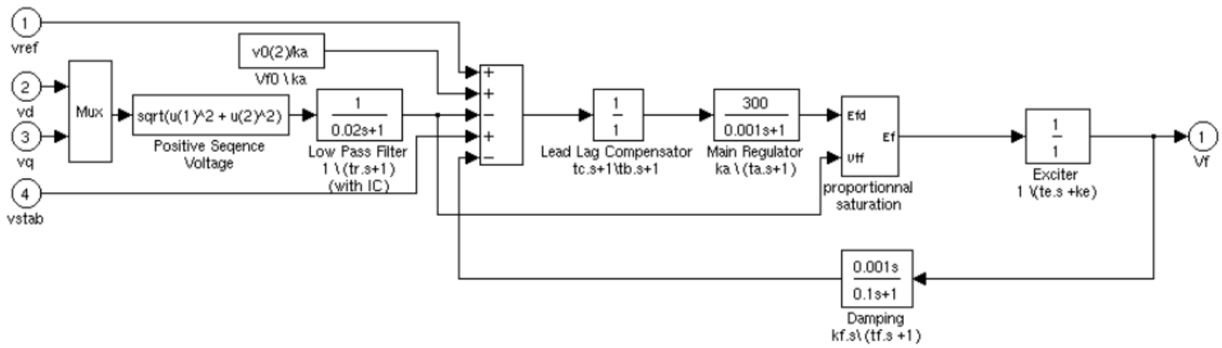


Figure 4.2: Simulink AVR Exciter Block Diagram

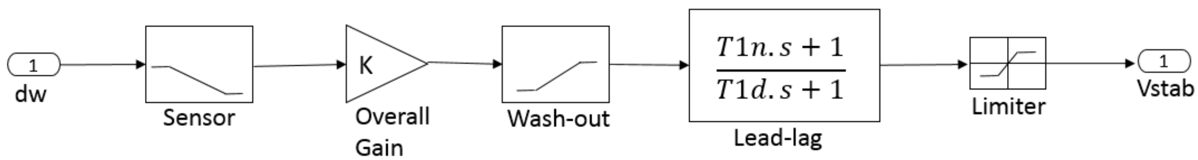


Figure 4.3: Simulink PSS Block Diagram

The model was executed with PSS and without. The model include startup of the equipment with 2 kW of load, increase to 4 kW of load, and decrease to 2 kW of load. Notice the oscillations observed in Figures 4.4 and 4.5. PSS greatly reduced the oscillations amplitude and duration.

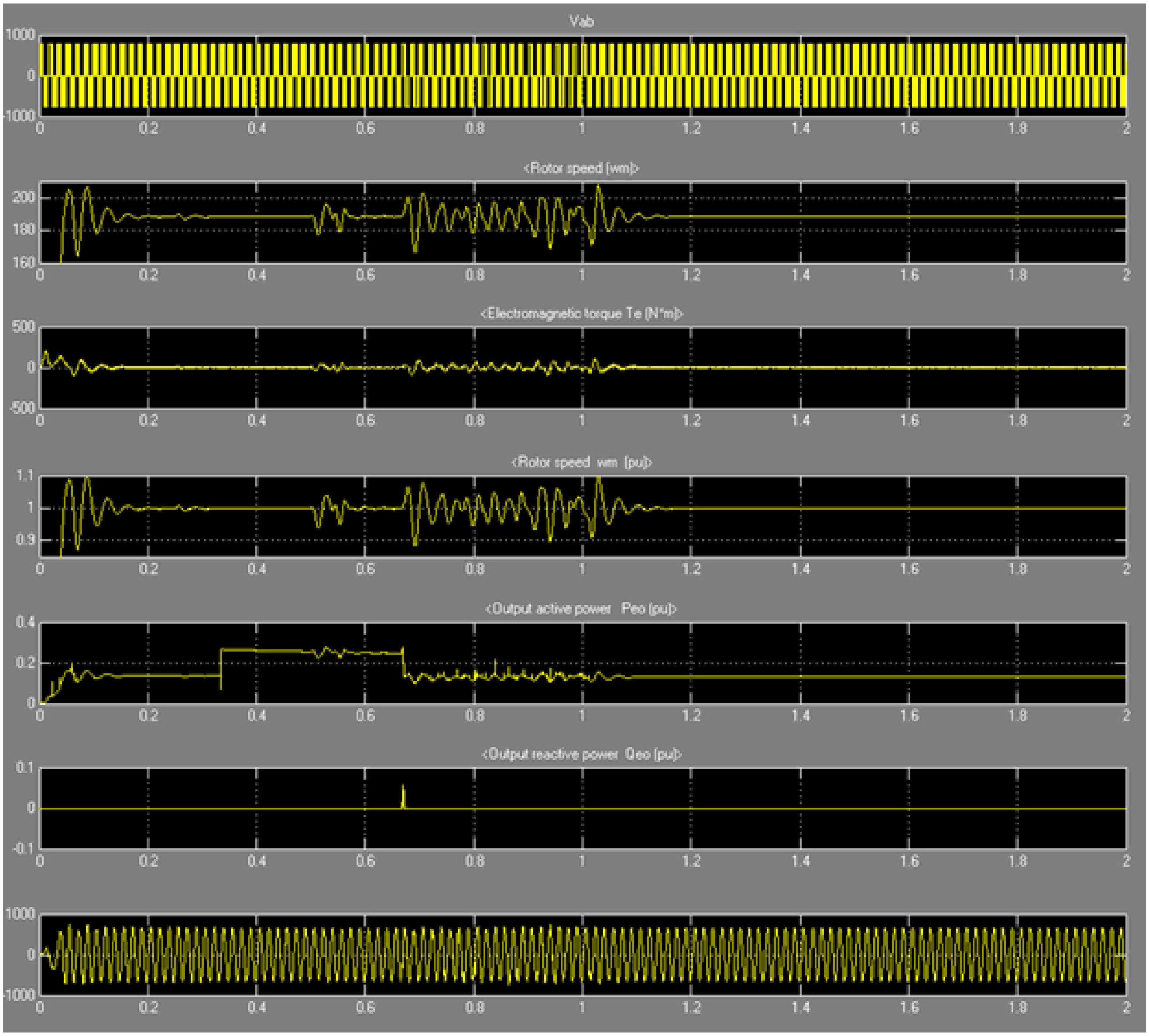


Figure 4.4: Simulink Simulation without PSS (Graphs arranged top to bottom: VFD Vab, Rotor Speed (Wm), Electromagnetic Torque (Nm), Rotor Speed (pu), Output Active Power (pu), Output Reactive Power (pu), Generator Vab)

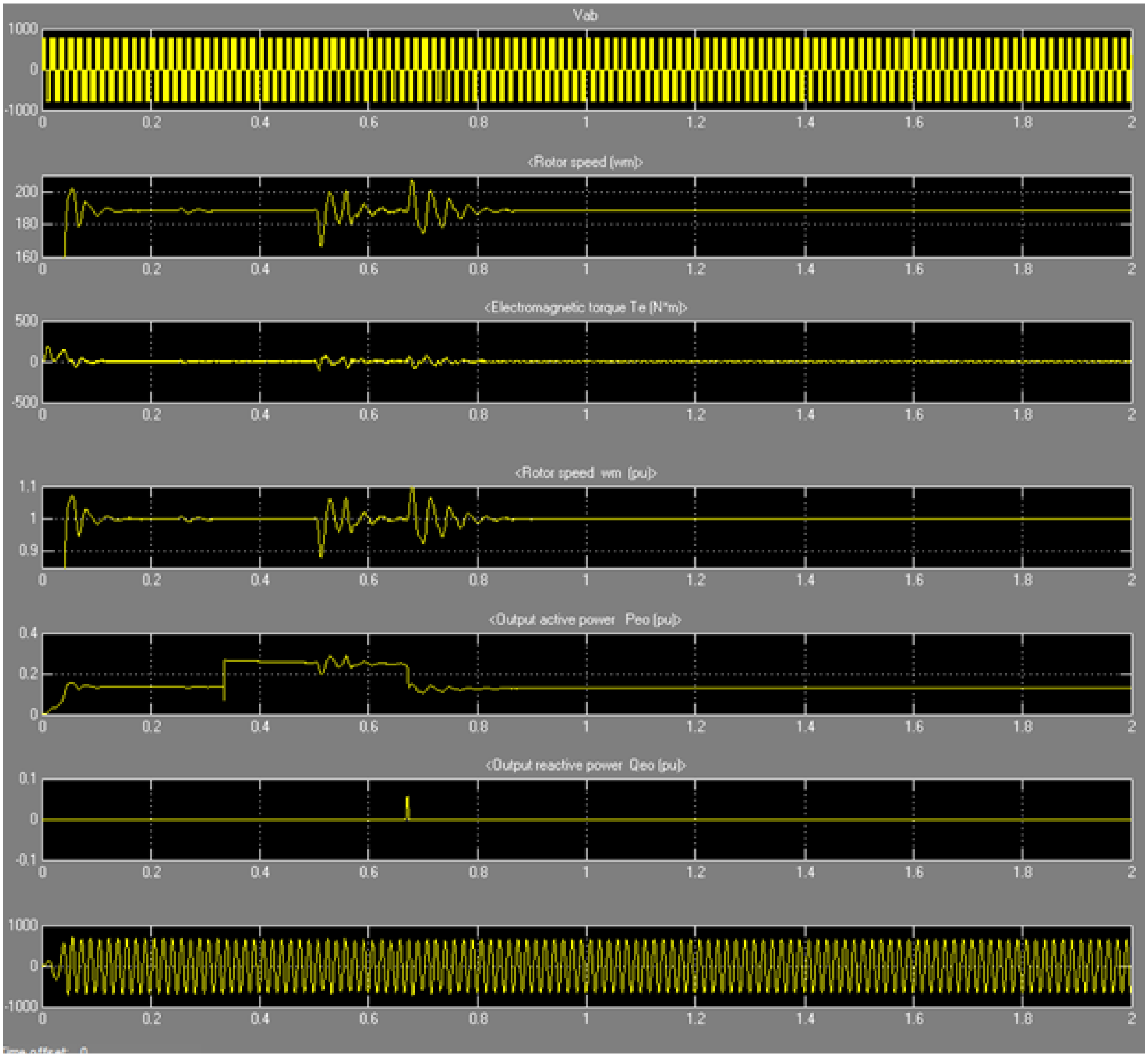


Figure 4.5: Simulink Simulation with PSS (Graphs arranged top to bottom: VFD Vab, Rotor Speed (Wm), Electromagnetic Torque (Nm), Rotor Speed (pu), Output Active Power (pu), Output Reactive Power (pu), Generator Vab)

## 4.2 Physical Model

The lab was used to perform a physical model for the network described in section 3.5. The VFD was operated at 60.07 Hz in to allow for slip caused by the induction motor. The generator was connected to a static load bank operating unsynchronized from the public grid. The load bank was set to 2 KW and an additional 4 KW was momentarily added to create system disturbances.

Figure 4.6: Load Bank

PSS was implemented via dSPACE. dSPACE utilized an encoder input and delivered an analog output voltage to the voltage regulator to adjust the gain function. Trends were recorded in dSPACE at a sampling rate of 10 kHz.

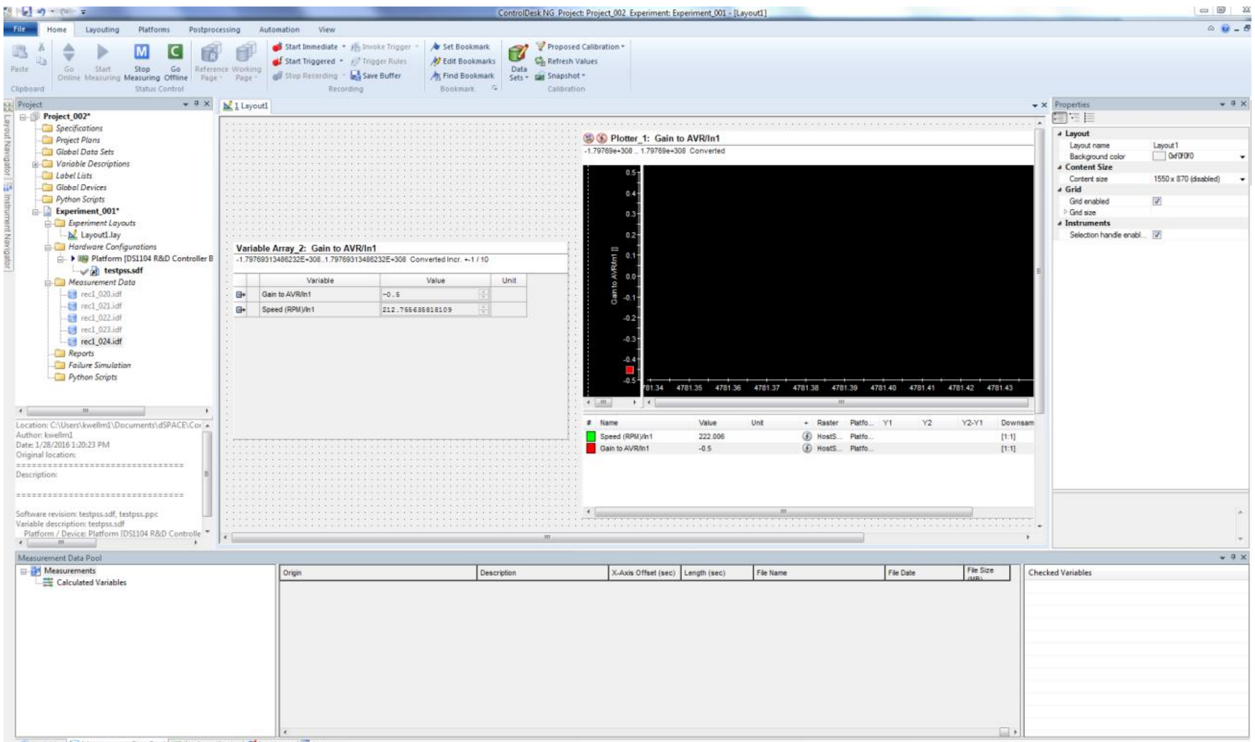


Figure 4.7: dSPACE Control Graphic

The generator was operated to observe the impact of PSS on the lab setup. At light loads, the encoder output fluctuated, which were possibly caused by rotor dynamics. Once additional load was added the effects decreased. Figures 4.8 and 4.9 shows the impact of PSS. Observe how the speed was held closer to desired 1800 rpm when PSS was utilized and oscillations were of lower frequency.

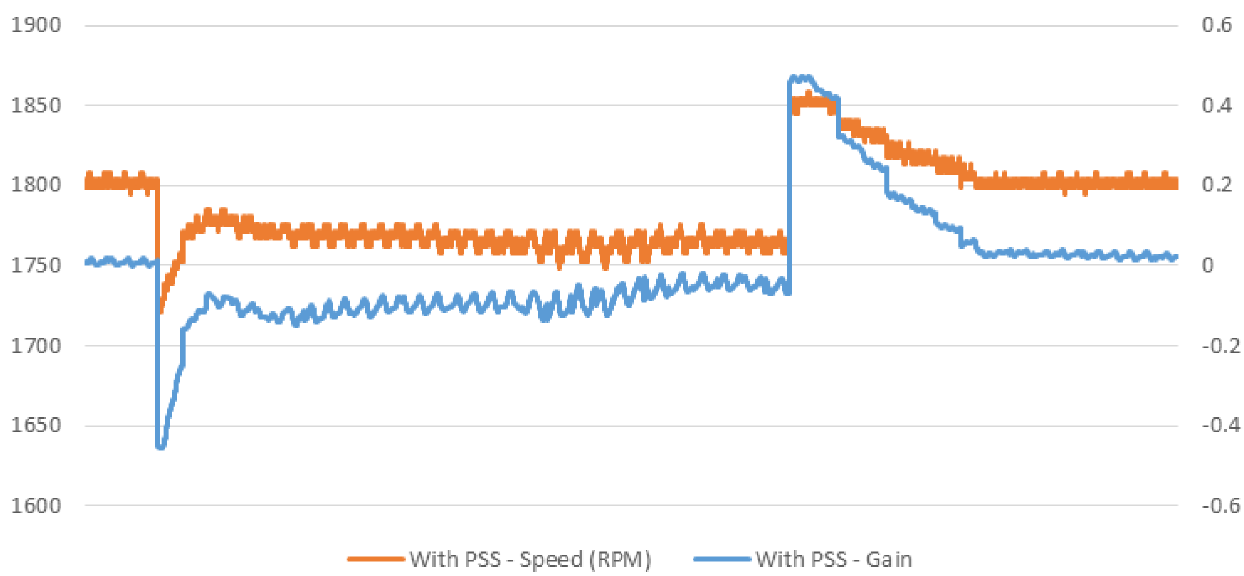


Figure 4.8: Generator Speed and Gain with PSS Implemented

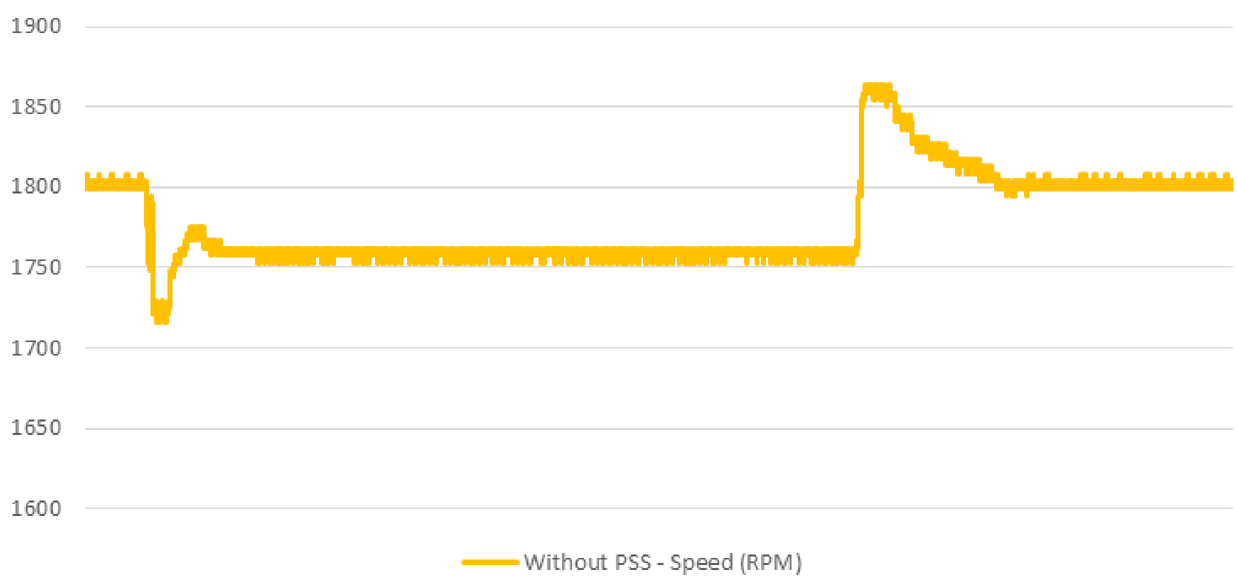


Figure 4.9: Generator Speed without PSS Implemented

To better observe the characteristics of PSS, we must observe the points of interest more closely. Figure 4.10 is a capture of load suddenly added to the generator. Since PSS is reactive to disturbances rather than proactive, the speed will sharply decrease for both cases.

Notice the speed is maintained higher when PSS is used and the recovery time from the event is much quicker. Figure 4.11 shows the impact of suddenly removing load from the generator. Notice that the speed to kept lower when PSS is utilized and the response time is slightly quicker.

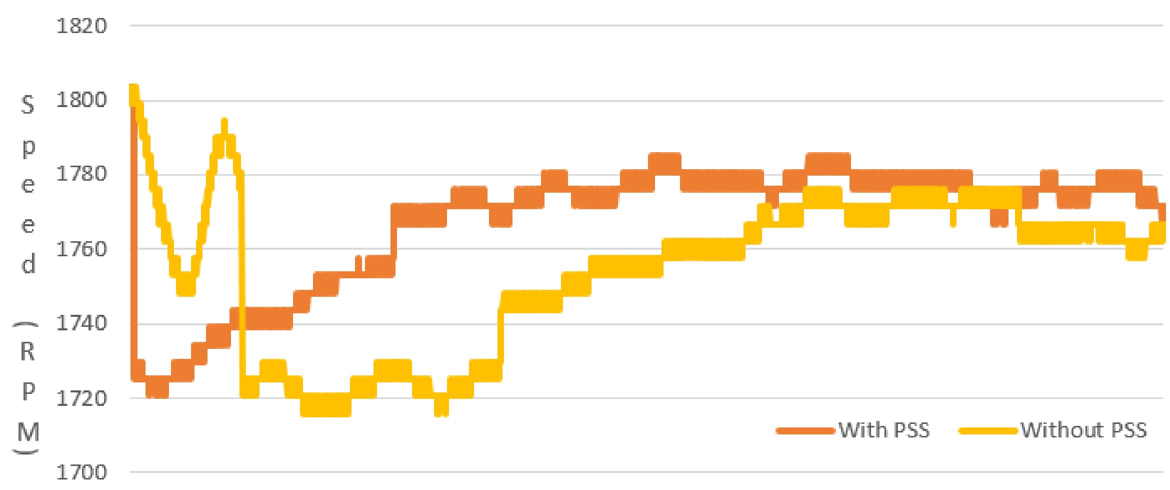


Figure 4.10: Speed versus Time with and without PSS with Increasing Load

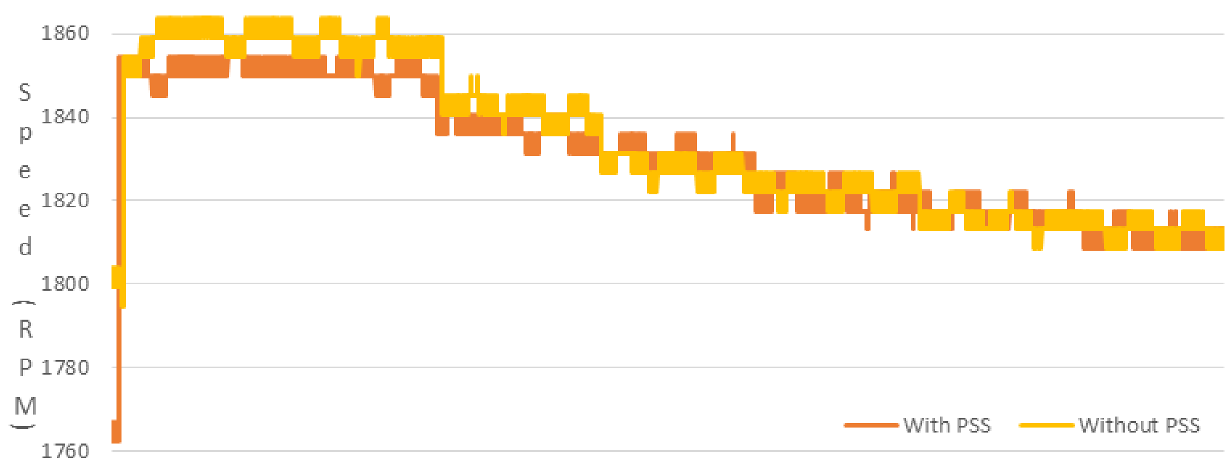


Figure 4.11: Speed versus Time with and without PSS with Decreasing Load

### 4.3 Conclusion

The lab performed well under a purely resistive load. All tests were perform in isochronous mode, but the system was synchronized on several occasions for other experiments. PSS was originally to be run through a National Instruments controller. Due to IT issues with driver and lack of training on the software, dSPACE was utilized instead. Future experiments will require a high inertia constant kVA load, such as an induction motor. Load can be controlled by driving a blower with an air dampener.

On several occasions, the generator was synchronized to the grid through a three-phase contactor. Generator protective relay performed the synchronizing check function to ensure the systems where in synchronization. VFD was changed to torque mode to allow finer tuning of the load. Load was successfully varied from full motoring to full generation. However, one phase was operating at a much higher current. This is likely due to high loading on that specific phase in the Electrical Engineering building. A system operating in isochronous mode has much larger impedance than grid.

# CHAPTER 5: SUMMARY

LSU Power Systems Lab was designed to handle a variety of experiments. These experiments can be performed with software or physical components. The lab can operate on-grid or off-grid, and loads can easily be changed. Generator parameters can be modified to best replicate the study's needs. This project challenged me greatly, and I have learned a lot.

## REFERENCES


[1] Shahab Mehraeen, S. Jagannathan, Mariesa L. Crow, “Novel Dynamic Representation and Control of Power Systems With FACTS Devices”, IEEE Transactions on Power Delivery, Vol 25 No 3, pp. 1542-1554

[2] Shahab Mehraeen, S. Jagannathan, Mariesa L. Crow, “Power System Stabilization Using Adaptive Neural Network-Based Dynamic Surface Control”, IEEE Transactions on Power Delivery, Vol 26 No 2, pp. 669-680

[3] Basler Electric, *Instruction Manual for Digital Excitation Control System DECS-250*, July 2013

[5] Basler Electric, *Instruction Manual for BE1-11g Generator Protection System*, February 2017

[6] Yaskawa, *G7 Drive Technical Manual*, July 2008

[7*] C.R. Mason, Art & Science of Protective Relaying* - Online Version: http://www.gegridsolutions.com/multilin/notes/artsci/index.htm

[8] *IEEE Guide for Synchronous Generator Modeling Practices and Applications in Power System Stability Analyses*, IEEE std 1110-2002, 2002

[9] *IEEE Recommended Practice for Excitation Models for Power System Stability Studies*, IEEE std 421.5-2016, 2016

[10] *IEEE Standard Definitions for Excitation Systems of Synchronous Machines*, IEEE std 421.1-2007, 2007

[11] Zia A Yamayee, Juan L. Bala, Jr., *Electromechanical Energy Devices and Power Systems*, John Wiley & Sons, Inc., 1994. pp. 221-438.

## APPENDIX: IEEE 14 Bus

Table A.1 IEEE 14 Bus - Load

| Bus | Voltage | PL | QL |
|---|---|---|---|
| 1 | 1.0600 | 0.0000 | 0.0000 |
| 2 | 1.0450 | 0.2170 | 0.1270 |
| 3 | 1.0100 | 0.9420 | 0.1900 |
| 4 | 1.0000 | 0.4780 | 0.0390 |
| 5.00% | 1.0000 | 0.0760 | 0.0160 |
| 5 | 1.0000 | 0.0000 | 0.0000 |
| 6 | 1.0700 | 0.1120 | 0.0750 |
| 7 | 1.0000 | 0.0000 | 0.0000 |
| 8 | 1.0900 | 0.0000 | 0.0000 |
| 9 | 1.0000 | 0.2950 | 0.1660 |
| 10 | 1.0000 | 0.0900 | 0.0580 |
| 11 | 1.0000 | 0.0350 | 0.0180 |
| 12 | 1.0000 | 0.0610 | 0.0160 |
| 13 | 1.0000 | 0.1350 | 0.0580 |
| 14 | 1.0000 | 0.1490 | 0.0500 |

Table A.2 IEEE 14 Bus - Line Impedance

| From Bus | To Bus | R | X | Y |
|---|---|---|---|---|
| 1.0000 | 2.0000 | 0.01938 | 0.05917 | 0.0528 |
| 1.0000 | 8.0000 | 0.05403 | 0.22304 | 0.0492 |
| 2.0000 | 3.0000 | 0.04699 | 0.19797 | 0.0438 |
| 2.0000 | 6.0000 | 0.05811 | 0.17632 | 0.0374 |
| 2.0000 | 8.0000 | 0.05695 | 0.17388 | 0.0340 |
| 3.0000 | 6.0000 | 0.06701 | 0.17103 | 0.0346 |
| 6.0000 | 8.0000 | 0.01335 | 0.04211 | 0.0128 |
| 6.0000 | 7.0000 | 0.00000 | 0.20912 | 0.0528 |
| 6.0000 | 9.0000 | 0.00000 | 0.55618 | 0.0492 |
| 8.0000 | 4.0000 | 0.00000 | 0.25202 | 0.0438 |
| 4.0000 | 11.0000 | 0.09498 | 0.19890 | 0.0374 |
| 4.0000 | 12.0000 | 0.12291 | 0.25581 | 0.0340 |
| 4.0000 | 13.0000 | 0.06615 | 0.13027 | 0.0346 |
| 7.0000 | 5.0000 | 0.00000 | 0.17615 | 0.0128 |
| 7.0000 | 9.0000 | 0.00000 | 0.11001 | 0.0528 |
| 9.0000 | 10.0000 | 0.03181 | 0.08450 | 0.0492 |
| 9.0000 | 14.0000 | 0.12711 | 0.27038 | 0.0438 |
| 10.0000 | 11.0000 | 0.08205 | 0.19207 | 0.0374 |
| 12.0000 | 13.0000 | 0.22092 | 0.19988 | 0.0340 |
| 13.0000 | 14.0000 | 0.17093 | 0.34802 | 0.0346 |

Table A.3 IEEE 14 Bus with Load Components Specified

| Voltage | PL (KW) | QL (KVAR) | R (Ω) | X(Ω) | L (H) | C (microF) |
|---|---|---|---|---|---|---|
| 254.4 | 0 | 0 | 0 | 0 | 0 | 0 |
| 250.8 | 1.562 | 0.914 | 40.259 | 68.789 | 0.182468 | 0 |
| 242.4 | 6.782 | 1.368 | 8.663 | 42.952 | 0.113933 | 0 |
| 240.0 | 3.442 | -0.281 | 16.736 | -205.128 | 0 | 12.931 |
| 240.0 | 0.547 | 0.115 | 105.263 | 500.000 | 1.326291 | 0 |

Table cont.

| | | | | | | |
|---|---|---|---|---|---|---|
| 240.0 | 0.000 | 0.000 | 0.000 | 0.000 | 0 | 0 |
| 256.8 | 0.806 | 0.540 | 81.779 | 122.123 | 0.32394 | 0 |
| 240.0 | 0.000 | 0.000 | 0.000 | 0.000 | 0 | 0 |
| 261.6 | 0.000 | 0.000 | 0.000 | 0.000 | 0 | 0 |
| 240.0 | 2.124 | 1.195 | 27.119 | 48.193 | 0.127835 | 0 |
| 240.0 | 0.648 | 0.418 | 88.889 | 137.931 | 0.365873 | 0 |
| 240.0 | 0.252 | 0.130 | 228.571 | 444.444 | 1.178926 | 0 |
| 240.0 | 0.439 | 0.115 | 131.148 | 500.000 | 1.326291 | 0 |
| 240.0 | 0.972 | 0.418 | 59.259 | 137.931 | 0.365873 | 0 |
| 240.0 | 1.073 | 0.360 | 53.691 | 160.000 | 0.424413 | 0 |

Table A.4 IEEE 14 Bus with Line Components Specified

| Bus | To Bus | R | L(mH) | C (microF) | C/2 (mF) |
|---|---|---|---|---|---|
| 1.0000 | 2.0000 | 0.155 | 1.2556 | 17.5070 | 8.754 |
| 1.0000 | 8.0000 | 0.432 | 4.7331 | 16.3134 | 8.157 |
| 2.0000 | 3.0000 | 0.376 | 4.2011 | 14.5229 | 7.261 |
| 2.0000 | 6.0000 | 0.465 | 3.7416 | 12.4008 | 6.200 |
| 2.0000 | 8.0000 | 0.456 | 3.6898 | 11.2735 | 5.637 |
| 3.0000 | 6.0000 | 0.536 | 3.6294 | 11.4724 | 5.736 |
| 6.0000 | 8.0000 | 0.107 | 0.8936 | 4.2441 | 2.122 |
| 6.0000 | 7.0000 | 0.000 | 4.4377 | 17.5070 | 8.754 |
| 6.0000 | 9.0000 | 0.000 | 11.8025 | 16.3134 | 8.157 |
| 8.0000 | 4.0000 | 0.000 | 5.3480 | 14.5229 | 7.261 |
| 4.0000 | 11.0000 | 0.760 | 4.2208 | 12.4008 | 6.200 |
| 4.0000 | 12.0000 | 0.983 | 5.4285 | 11.2735 | 5.637 |
| 4.0000 | 13.0000 | 0.529 | 2.7644 | 11.4724 | 5.736 |
| 7.0000 | 5.0000 | 0.000 | 3.7380 | 4.2441 | 2.122 |
| 7.0000 | 9.0000 | 0.000 | 2.3345 | 17.5070 | 8.754 |

Table cont.

| | | | | | |
|---|---|---|---|---|---|
| 9.0000 | 10.0000 | 0.254 | 1.7931 | 16.3134 | 8.157 |
| 9.0000 | 14.0000 | 1.017 | 5.7376 | 14.5229 | 7.261 |
| 10.0000 | 11.0000 | 0.656 | 4.0759 | 12.4008 | 6.200 |
| 12.0000 | 13.0000 | 1.767 | 4.2416 | 11.2735 | 5.637 |
| 13.0000 | 14.0000 | 1.367 | 7.3852 | 11.4724 | 5.736 |

## VITA

Kevin Daniel Wellman was born 1988, in Gulfport, MS. He received his Bachelor of Science from Mississippi State University in 2011. His career started in 2011 after graduation. He worked for The Dow Chemical Company as a Run Plant Engineer for Energy Systems in Plaquemine, LA from 2011 until 2015. In 2015, he transferred with the company to Houston, TX to become a site leverage Electrical Maintenance Engineer. He plans to be awarded the degree of Master of Science in Electrical Engineering in August of 2017.